Triple sensitivity amplification for ultrasensitive electrochemical detection of prostate specific antigen

Zhongxue Tang, Liyuan Wang, Zhanfang Ma

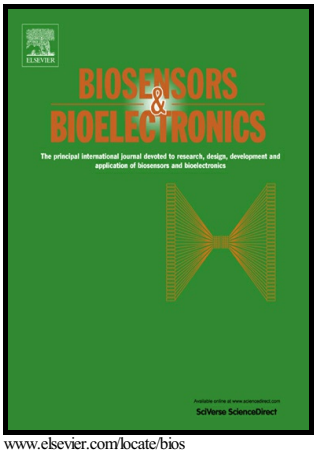

www.elsevier.com/locate/bios

PII: S0956-5663(16)31075-2
DOI: http://dx.doi.org/10.1016/j.bios.2016.10.057
Reference: BIOS9279

To appear in: *Biosensors and Bioelectronic*

Received date: 23 August 2016
Revised date: 20 October 2016
Accepted date: 20 October 2016

Cite this article as: Zhongxue Tang, Liyuan Wang and Zhanfang Ma, Triple sensitivity amplification for ultrasensitive electrochemical detection of prostat specific antigen, *Biosensors and Bioelectronic* http://dx.doi.org/10.1016/j.bios.2016.10.057

Triple sensitivity amplification for ultrasensitive electrochemical detection of prostate specific antigen

Zhongxue Tang, Liyuan Wang, Zhanfang Ma*

Department of Chemistry, Capital Normal University, Beijing 100048, China

mazhanfang@cnu.edu.cn

Abstract

In general, current difference (ΔI) due to immunoreactions is significant in determining biosensor sensitivity. In this work, a new strategy of triple sensitivity amplification for ultrasensitive electrochemical detection of prostate specific antigen (PSA) was developed. Au-poly(methylene blue) (Au-PMB) was implemented as a redox species with strong current signal at -0.144 V and used to fabricate the substrate of the biosensor. Conductive reduced graphene oxide-Au nanocomposites (Au-rGO) were coated on the Au-PMB modified glassy carbon electrode (GCE) to amplify current signal. After peptides (CEHSSKLQLAK-NH_2) were fixed on the Au-rGO/Au-PMB/GCE, the fixed peptides reacted with glutaraldehyde to immobilize polydopamine-Au-horse radish peroxidase nanocomposites (PDA-Au-HRP). The electrochemical sensing interface for PSA was realized. Due to smaller resistance compared to antibodies, the peptides which can be cleaved specifically by PSA were employed. After the incubation of PSA, a large ΔI was obtained and behaved as the decrease of current signal. Then the remaining PDA-Au-HRP accelerated an enzyme-catalyzed precipitation reaction between 4-chloro-1-naphthol and H_2O_2. A further decrease in current signal (namely the increase in ΔI) resulted from the poorly conductive precipitation adhering onto the biosensor. The designed biosensor presented a wide linear range from 1.0 fg mL^{-1} to 100 ng mL^{-1} with an ultralow

detection limit of 0.11 fg mL^{-1}.

Keywords: Au-poly(methylene blue), polydopamine-Au-HRP, peptide, prostate specific antigen, electrochemical biosensor, enzyme-catalyzed precipitation reaction

1. Introduction

Electrochemical analysis is commonly used due to its easy assembly, low-cost, rapid detection, and miniaturization (Zhu et al., 2015). This technique presents great advantages in determining analytes in complicated systems (Chikkaveeraiah et al., 2012; Bryan et al., 2013), especially in the detection of tumor biomarkers (Cui et al., 2008). The ultrasensitive and high selective determination of tumor biomarkers is urgent and important for early cancer diagnosis, which is meaningful to prolong the survival time (DeSantis et al., 2013; Jemal et al., 2011). Up to now, various electrochemical immunosensors have been reported, such as amperometric (Rong et al., 2016), potentiometric (Tang et al., 2006), and impedimetric (Akter et al., 2015) immunoassay. Among these methods, amperometric immunoassay has attracted much attention for its high sensitivity, low detection limit, and minimal determination time (Liu et al., 2016).

Conventional electrochemical immunoassay is based on the immune recognition relationship between antibodies and antigens (Fernandes et al., 2015; Zhai et al., 2016). Its sensitivity is tightly related to the difference of current signal (ΔI) which is caused by the recognized analytes (Liu et al., 2013) and significantly affected by the conductivity of immunosensor. However, conductivity of an electrochemical immunosensor significantly decreases when incubating with antibodies and blocking

reagents owing to their poor conductivity (Gao et al., 2013; Fernandes et al., 2013). This decrease in conductivity results in smaller ΔI and lowers the sensitivity. Hence, discovery an effective method to enhance sensitivity is necessary.

For label-free electrochemical immunosensor, the substrate commonly contained redox species (redox substrate), which can provide current signal. Apparently, in label-free immunoassay, ΔI is from the decrease of the current signal of biosensor after the treatment with antigen. Redox substrates are constructed by gathering redox species through electrodeposition (Kaushik et al., 2013), electrostatic adsorption (Rong et al., 2015), π-π stacking interactions (Gao et al., 2016) and coordination (Ou et al., 2008). If the current signal of the biosensor decreases to be zero by incubating antigen, the maximum value of ΔI and the highest sensitivity will be realized. However, after the incubation of antigens, the current signals of the immunosensors are still strong. This indicates that the current signal of the redox substrate has more space to decrease and the sensitivity would be further enhanced. In this case, an effective method to promote the current decrease is essential for elevating the sensitivity of label-free electrochemical sensors.

Prostate specific antigen (PSA) has proven to be a classic biomarker for prostatic carcinoma screening, diagnosis monitoring, and therapy evaluation (Nam et al., 2003; Mohan et al., 2013; Gao et al., 2013), and has been investigated as a possible marker for breast cancer in women (Walsh et al.,2010). Hence, the ultrasensitive determination of PSA is significant. Herein, a new strategy of triple sensitivity amplification for the ultrasensitive electrochemical detection of PSA was developed. In this work, Au-poly(methylene blue) (Au-PMB) was easily synthesized by oxidative polymerization of methylene blue (MB) and used as a novel redox species with strong current signal at -0.144V. The redox substrate was constructed by Au-PMB and

covered by reduced graphene oxide-Au nanocomposites (Au-rGO). The peptides with specific amino acid sequences were immobilized on the substrate, which can be specifically cleaved by PSA (Jung et al., 1992; Zhao et al., 2010). Polydopamine-Au-HRP (PDA-Au-HRP) nanocomposites were chemically linked with peptides by using glutaraldehyde. Thus, the biosensor was obtained. This strategy possessed three advantages. First, Au-rGO can improve the conductivity of biosensor resulting in signal amplification and offer active sites for immobilizing the peptides. Second, the peptides just slightly hinder the electron transfer on the sensing interface (Mahshid et al., 2015). Third, after incubating with PSA, the remaining PDA-Au-HRP was employed to accelerate an enzyme-catalyzed precipitation reaction between 4-chloro-1-naphthol (4-CN) and H_2O_2 (Akter et al., 2015) to produce insoluble benzo-4-chlorohexadienone, resulting in a significant signal decrease and a larger ΔI. The proposed biosensor exhibited a wide linear range with an ultralow detection limit for PSA. For human serum detection, the results of the biosensor showed great accordance with these of the enzyme-linked immunosorbent assay (ELISA), indicating its potential in clinical diagnosis.

2. Experimental

2.1. Reagents and materials

HRP, PSA, anti-PSA, human immunoglobulin G (IgG), carcinoembryonic antigen (CEA) and alpha-fetoprotein (AFP) were purchased from Shanghai Linc-Bio Science Co. Ltd. (Shanghai, China). The specific peptide (CEHSSKLQLAK-NH_2) was purchased from Shanghai Sangon (Shanghai, China). GO was obtained from Nanjing JCNANO Tech Co. Ltd (Nanjing, China). MB was obtained from Tianjin Guangfu Fine Chemical Research Institute (Tianjin, China). Dodecyltrimethylammonium bromide (DTAB), ascorbic acid (AA, 99.7%), dopamine hydrochloride (DA, 99%),

uric acid (UA), $HAuCl_4 \cdot 3H_2O$ (99.99%), D-(+)-glucose (GLU), 4-chloro-1-naphthol (4-CN), dopamine hydrochloride and bovine albumin (BSA, standard grade) were commercially obtained from Alfa Aesar (Tianjin, China). Clinical human serum samples were provided by Capital Normal University Hospital (Beijing, China). All other reagents were used as received.

2.2. Apparatus

Deionized water was purified through an Olst ultrapure K8 apparatus (Olst, Ltd., resistivity >18 MΩ cm). Transmission electron microscopy (TEM) measurements were performed with a JEOL-100CX electron microscope (Hitachi, Japan) under 80 kV accelerating voltage (H7650, Hitachi, Japan). Scanning electron microscopy (SEM) measurements were performed with a Hitachi S-4800 scanning electron microscope. X-ray photoelectron spectroscopy (XPS) analysis was performed on an Escalab 250 X-ray photoelectron spectroscope (Thermofisher, American). Ultraviolet-visible (UV-vis) spectroscopy measurements were performed on a UV-2550 UV-vis spectrophotometer (Shimadzu, Japan). Fourier transform infrared (FTIR) spectra were recorded on a VECTORTM 22 spectrometer (Bruker). Zeta potential measurements were performed on a Zetasizer Nano ZS (Malvern Instruments Co., UK). Square wave voltammetry (SWV) measurements were conducted with a CHI 832 electrochemical workstation (Shanghai Chenhua Instruments Co., LTD, China). The three-electrode system consisted of a modified glassy carbon electrode (GCE) as the working electrode, a platinum wire as the counter electrode, and an Ag/AgCl electrode saturated with KCl as the reference electrode.

2.3. Synthesis of Au-PMB

After a homogeneous solution was produced by mixing 1.00 mL 10.00 mM MB, 3.00 mL ultrapure water and 3.00 mL 2.0 mM DTAB aqueous solution, 200 μL 4.0%

$HAuCl_4$ aqueous solution was quickly injected into the mixture with stirring for 1 min. The mixture immediately became dark blue. Followed, the obtained mixture kept ageing for 6 hours at room temperature. Au-PMB composites were collected by centrifugation, washed by water for several times, and diluted with water to 2.00 mL.

2.4. Synthesis of PDA-Au-HRP

PDA nanoparticles were synthesized according to a literature (Ju et al., 2011). In brief, after 18.0 mg dopamine hydrochloride was added to 50°C 9.00 mL water, 76 μL 1.0 M NaOH aqueous solution was immediately injected into the above solution and kept reacting for 5 h with stirring. PDA nanoparticles were centrifuged, washed and dispersed into 0.50 mL water. Then, the 0.50 mL PDA solution was mixed with 1.20 mL 0.20 M sodium citrate aqueous solution and 0.30 mL water, and then the mixture was quickly injected into 25.00 mL 0.02% boiling $HAuCl_4$ aqueous solution with vigorous stirring for 2 h. Finally, PDA-Au was centrifuged, thoroughly washed and diluted with water to 5.00 mL.

For loading HRP, 2.00 mL PDA-Au was mixed with 4.00 mL 1.0 mg mL^{-1} HRP and 2.00 mL water with mildly stirring for 6 h. Then, BSA solution was added to block the unreacted active sites with stirring for 1 h. After that, PDA-Au-HRP-BSA was centrifuged, thoroughly washed, diluted to 8.00 mL by water and then stored at 4°C.

2.5. Synthesis of Au-rGO

The Au-rGO was produced by the citrate-mediated reduction of $HAuCl_4$ and GO (Peng et al., 2012). 4.00 mL 1.0 mg mL^{-1} GO aqueous solution was added into 25.00 mL 0.05% $HAuCl_4$ aqueous solution drop by drop, and kept stirring for 2 h. After that, 1.20 mL 0.20 M sodium citrate aqueous solution was added into the obtained mixture and stirred for 1h, and then the mixture was heated reflux for 1 h. After the obtained

solution cooled down to room temperature, Au-rGO was centrifuged, thoroughly washed and diluted with water to 8.00 mL.

2.6. Preparation of the sensing platform

GCE was carefully polished with 0.05 μm alumina powders and followed by successively sonication washing with water and ethanol, respectively. Then, 20 μL Au-PMB and 20 μL Au-rGO were subsequently dropped on the GCE surface. 80 μL 50 mM peptide (CEHSSKLQLAK-NH_2) was incubated on Au-rGO/Au-PMB/GCE for 1 h, and was activated by 50 μL 0.10% glutaraldehyde for 30 min. After that, 50 μL PDA-Au-HRP-BSA was incubated on the modified electrode for 1h. Then PDA-Au-HRP-BSA/peptides/Au-rGO/Au-PMB/GCE was obtained and stored at 4°C. After each step, the modified GCE was carefully washed by ultrapure water.

2.7. Electrochemical measurement

PDA-Au-HRP-BSA/peptides/Au-rGO/Au-PMB/GCE was incubated with 80 μL PSA for 1 h and then washed with ultrapure water. After that, the obtained PDA-Au-HRP-BSA /peptides/Au-rGO/Au-PMB/GCE was dipped in 1.0 mM 4-CN solution containing 1.0 mM H_2O_2 for 30 min. Subsequently, the SWV measurement was conducted from -1.0 V to 0.4 V in 0.10 M PBS (pH 7.0) with pulse amplitude of 25 mV and an increase of potential of 4 mV s^{-1}.

3. Results and discussion

3.1. Principle of the proposed label-free electrochemical biosensor

Generally, the redox species were classified into inorganic redox and organic species, such as Pb^{2+} and MB (Rong et al., 2016; Wang et al., 2010; Santos et al., 2015). In consideration of their current signal intensity and toxicity for proteins (Sipos et al., 2016), these redox species were gathered and firmly fixed before detecting biomarkers. The application of functional materials and extra experiments were

complicated and time-consuming for immobilizing these redox species. Oxidative polymerization offered a new method to synthesize new conductive polymers (Zhai et al., 2013; Wang et al., 2016) in which implementing a polymerized organic redox molecule as the redox species avoided the complicated gathering process and fixing procedure.

The fabrication procedure and detection principle of the proposed biosensor for PSA were illustrated in Scheme 1. Au-PMB was synthesized by the oxidative polymerization of MB using $HAuCl_4$ as an oxidizing agent and used to fabricate the redox substrate. Signal enhancement was initially achieved by coating Au-PMB/GCE with Au-rGO, which greatly accelerated the electron transfer. ΔI was then amplified by replacing anti-PSA with the specific peptide. In comparison to antibodies, peptides with smaller molecular weight slightly hinder the electronic transfer on the sensing interface. Finally, ΔI amplification procedure was conducted using PDA-Au-HRP-BSA to accelerate an enzyme-catalyzed precipitation reaction, which behaved as a large current signal decrease. Through the triple sensitivity amplification method, the presented biosensor was capable of ultrasensitive determination of PSA.

Scheme 1

3.2. Characterizations of Au-PMB, Au-rGO, and PDA-Au

The morphologies and sizes of Au-PMB, Au-rGO, PDA-Au and PDA were identified by TEM analysis (Fig. 1**A**-**D**). MB was employed by oxidative polymerizition for its electrochemical activity (Gorle et al., 2016). The as-prepared Au-PMB was micron-sized and stick-like nanocomposites with a rough surface (Fig. 1**A**). Au-rGO sheets were synthesized by in situ generation of Au nanoparticles, which were approximately 7±1.5 nm in diameter and densely distributed on rGO (Fig. 1**B**). The PDA nanoparticles displayed homogeneous morphology and were about

200±20 nm in size (Fig. 1**C**). For PDA-Au nanocomposites, Au nanoparticles were densely coated onto the as-prepared PDA nanoparticles (Fig. 1**D**).

Fig. 1

The detailed compositions of Au-PMB, Au-rGO, PDA, and PDA-Au were characterized by XPS (Fig. 1**E**-**H**, Table S1). As shown in Fig. 1**E**, the C1s, O2p, S2p, and N1s peaks corresponded to MB. For Au-rGO, the C1s and O2p peaks belongs to elements present in rGO (Fig. 1**F**). For PDA-Au, the C1s, O2p, and N1s peaks were designated to dopamine (Fig. 1**G**,**H**). The Au4f peaks of Au-PMB, Au-rGO, and PDA-Au were assigned to reduced gold nanostructures (Fig. 1**E, F, H**) (Liu et al., 2013). The $Au4d_{3/2}$ peaks at about 335 eV and $Au4d_{5/2}$ peaks at about 350 eV of Au-PMB and PDA-Au corresponds to Au (Fig. 1**E**,**H**) (Fuggle et al., 1977; Turner et al., 1990). Then, Au-PMB, Au-rGO, and PDA-Au were further characterized by UV-Vis spectroscopy (Fig. S1**A-C**), and two absorption peaks at 663 nm and 614 nm were observed for MB (Fig. S1**A**) (Mellish et al., 2002). In contrast, no special absorption peaks were observed in the visible region for GO (Fig. S1**B**) or PDA (Fig. S1**C**). For Au-PMB, Au-rGO, and PDA-Au, obvious peaks were noticed at 530 nm, 575 nm, and 560 nm, respectively, resulting from the surface plasma resonance of gold nanoparticles (Xianyu et al., 2014).

FTIR measurements were performed in order to characterize the structural analysis of Au-PMB, Au-rGO, and PDA-Au (Fig. S1**D**-**F**). The peak at 2980 cm^{-1} was derived from the C-H bond, and the peak over 3000 cm^{-1} was from the active H in $-NH_2$ (Fig. S1**D**), -COOH (Fig. S1**E**), and -OH groups (Fig. S1**E**,**F**). The peaks around 1460-1650 cm^{-1} corresponded to conjugated structures, including benzene and heterocyclic conjugated groups. In addition, the zeta potentials of Au-PMB, Au-rGO, and PDA-Au were illurstrated in Fig. S2 and suggested that the Au-PMB was

positively charged as a result of MB and DTAB (Mellish et al., 2002). In contrast, Au-rGO was negatively charged owing to GO and the sodium citrate modified gold nanoparticles. The π-π stacking and electrostatic adsorption promoted Au-rGO to adhere onto Au-PMB. In approxmately neutral pH system (~pH 7), PDA-Au was negatively charged mainly due to the deprotonation of the phenolic groups of PDA (Liu et al., 2014).

3.3. Stepwise construction procedures of the biosensor

The stepwise construction procedures of the biosensor were monitored by SWV measurements (Fig. 2**A**). A high current signal (-0.144 V, 587.7 μA) was produced by the Au-PMB-modified GCE (curve a) and then enhanced by covering Au-rGO for the great specific surface area and excellent conductivity of Au-rGO (curve b). After that, the signal decreased after peptides were incubated on the Au-rGO/Au-PMB/GCE (curve c), indicating that the peptide was successfully immobilized. The signal decrease was caused by the peptide-hindered electron transport. Conversely, the peak current increased when the PDA-Au-HRP-BSA /peptides/Au-rGO/Au-PMB/GCE was treated with glutaraldehyde and PDA-Au-HRP-BSA (curve d), suggesting that the conductivity of the modified electrode was improved by the fixed PDA-Au-HRP-BSA. After incubating PSA, the peak current decreased (curve e), but the obtained signal was stronger than that in curve c, indicating that the peptide was cleaved by PSA, and ΔI of 23.4 μA was obtained. The current signal decreased further after the oxidation and precipitation of 4-CN, due to poor conductivity of benzo-4-chlorohexadienone (curve f). In contrast, the biosensor without PSA produced a lower current peak (150.0 μA, curve g), which was defined as the blank signal, following the enzyme-catalyzed precipitation reaction. In this case, ΔI turned to be the current signal difference between curve f and g, increasing from 23.4 μA to 167.8 μA.

Compared with curve g, curve f demonstrates that the peptides were successfully cleaved and PDA-Au-HRP-BSA was cut off by PSA. While electrochemical impedance spectroscopy measurements results for the fabrication procedures of this biosensor were illustrated in the supplementary information (Fig. S3).

To investigate the immunosensing procedures of the PDA-Au-HRP-BSA/peptides/Au-rGO/Au-PMB/GCE for PSA in more detail, SEM images were taken. The homogeneous stick-like Au-PMB (Fig. 2**B**) and PDA-Au (Fig. 2**C**) were well dispersed. PDA-Au-HRP-BSA nanocomposites were densely scattered onto the surface of PDA-Au-HRP-BSA/peptides/Au-rGO/Au-PMB/GCE (Fig. 2**D**). In comparison, PDA-Au-HRP-BSA nanocomposites were slightly scattered after the PDA-Au-HRP-BSA/peptides/Au-rGO/Au-PMB/GCE was incubated with PSA (Fig. 2**E**), suggesting that the peptides were cleaved and an abundance of PDA-Au-HRP-BSA nanocomposites were cut off. PDA-Au-HRP-BSA was coated after the precipitation reaction, indicating that the insoluble benzo-4-chlorohexadienone was firmly affixed onto the surface of the modified electrode (Fig. 2**F**).

Fig. 2

3.4. Optimization of detection conditions

Peptides are an important factor for the sensitivity of the biosensor. According to previous literature, the best immobilization time of peptides was found to be 1 h (He et al., 2015). To further investigate peptide influence, optimization of the quantity of peptides was carried out (Fig. S4**A**). The current signal gradually decreased with the increas**e** of peptide concentration from 10 μM to 30 μM, which may be explainable to peptides as organic molecule hindering the electron transfer on the surface of GCE. Then the current signal remained constant when the concentration further increased

from 30 μM to 50 μM, indicating the saturated adsorption of peptides. To avoid nonspecific adsorption, 50 μM peptide was chosen for the subsequent experiments. Then, the incubation time for 50 μM peptide was optimized (Fig. S4**B**). The signal of the biosensor was decreased gradually by extending the incubation time from 10 min to 40 min. At 40 min, the signal remained constant, indicating that the peptide was successfully fixed; thus, 40 min was chosen as the incubation time for the peptide.

The precipitation reaction time is also a significant parameter for the analytical performance of the biosensor. When the precipitation reaction time increased to 30 min, the electrochemical signal obviously decreased due to the precipitation hindering electron transfer. With the further increase of the precipitation reaction time, HRP could be completely covered by the benzo-4-chlorohexadienone. In this case, the precipitation reaction was ceased and the current signal remained constant (Fig. S4**C**). Therefore, 30 min of precipitation reaction time was used in following experiments.

The electrochemical signal was significantly influenced by the pH of the analyzed solution. After the oxidation and precipitation of 4-CN, a weaker signal was observed from the biosensor incubated with PSA (Fig. S4**D**), indicating that benzo-4-chlorohexadienone hindered the electron transfer. ΔI gradually increased when pH increased 5.5 to 7.0, and then decreased when pH changed from 7.0 to 7.5. Thus, pH of 7.0 for PBS was chosen for the following experiments.

3.5. Analytical performance of the biosensor

Under the above optimal conditions, the PDA-Au-HRP-BSA /peptides/Au-rGO/Au-PMB/GCE were incubated with a series of PSA (Fig. 3**A**). The as-prepared biosensor exhibited a wide detectable linear range from 1 fg m L^{-1} to 100 ng mL^{-1}, and the blank signal was shown in Fig. 2**A** (curve g) and 3**A** (curve 0). The ultralow detection limit of this biosensor was 0.11 fg mL^{-1} for PSA at a

signal-to-noise ratio of 3σ (S/N = 3) (σ is the standard deviation of signal in a blank solution) (Fig. 3**B**). The linear equation was $\Delta I=16.97\log_{10}C+133.9$, where R^2 was 0.996.

Compared to some recent literature, the proposed biosensor exhibited a wider linear detection range (LDR), a lower limit of detection (LOD), and a higher sensitivity for PSA (Table S2). Generally, the LDR was two orders of magnitude wider, and LOD was two orders of magnitude lower than the recent works.

Fig. 3

3.6. Evaluation of repeatability, specificity and stability of the biosensor

Under the optimal conditions, the repeatability, specificity and stability of the biosensor were evaluated. In order to investigate repeatability, the prepared biosensors were used to perform parallel experiments. The 100 ng mL^{-1}, 1 ng mL^{-1}, 100 pg mL^{-1}, 1 pg mL^{-1}, and 100 fg mL^{-1} PSA were determined, and standard deviations (5.9%, 5.7%, 3.3%, 4.6% and 6.6%) suggest that this electrochemical assay possessed good repeatability. To address specificity, samples of 10 ng mL^{-1} PSA mixed with 100 ng mL^{-1} disturbance substances (AA, DA, UA, GLU, BSA, AFP, CEA, and IgG) were analyzed. The current signals vibration between the results for each PSA samples was negligible, demonstrating the proposed electrochemical assay displays excellent specificity (Fig. S5, Table S3). To investigate the stability, the PDA-Au-HRP-BSA/peptides/Au-rGO/Au-PMB/GCE was stored at 4°C and then the analytical capacity of the proposed biosensors for PSA was evaluated three times a week. After 35 days, compared to the freshly prepared biosensor, the changes in peaks were negligible and its initial response for PSA retained more than 95% of its initial value (Fig. S6, Table S4), indicating the good stability of the biosensor.

3.7. Analysis of clinical serum samples

To investigate the reliability of the proposed method, ELISA was employed as a standard method. Investigation of ten serum samples was performed via ELISA and the proposed method. Each human serum sample was analyzed three times. The results were listed in the Table S5.The relative error between ELISA and the proposed method was less than 10%, indicating that this biosensor possessed good reliability.

4. Conclusion

In summary, a triple sensitivity amplification strategy was developed for ultrasensitive electrochemical determination of PSA. In order to build a redox substrate with powerful electrochemical signal, Au-PMB was synthesized as a novel redox species via oxidative polymerization. To enlarge ΔI, the electrochemical signal was enhanced by Au-rGO, and then peptides that specifically recognize PSA were used instead of anti-PSA. Further, the ΔI increased to 167.5 μA primarily due to the enzyme-catalyzed precipitation reaction. The proposed electrochemical assay presents a wide linear range, low detection limit, and high sensitivity. For clinical serums, the proposed assay agreed well with ELISA. This work presents a new strategy to make full use of the signal of the redox substrate in the label free electrochemical biosensor for determining targets.

Acknowledgments

This research was financed by grants from the National Natural Science Foundation of China (21273153, 21673143), Beijing Natural Science Foundation (2132008), and the Project of the Construction of Scientific Research Base by the Beijing Municipal Education Commission.

References

Akter, R., Rhee, C.K., Rahman, M.A., 2015. Biosens. Bioelectron. 66, 539-546.

Bryan, T., Luo, X.L., Bueno, P.R., Davis, J.J., 2013. Biosens. Bioelectron. 39, 94-98.

Chikkaveeraiah, B.V., Bhirde, A.A., Morgan, N.Y., Eden, H.S., Chen, X.Y., 2012. ACS Nano 6, 6546-6561.

Cui, R.J., Liu, C., Shen, J.M., Gao, D., Zhu, J.J., Chen, H.Y., 2008. Adv. Funct. Mater. 18, 2197-2204.

DeSantis, C., Naishadham, D., Jemal, A., 2013. Ca Cancer J. Clin. 63, 151-166.

Gorle, D. B., Kulandainathan, M. A., 2016. RSC Adv. 6, 19982-19991.

Fernandes, F.C.B., Patil, A.V., Bueno, P.R., Davis, J.J., 2015. Anal. Chem. 87, 12137-12144.

Fernandes, F.C.B., Góes, M.S., Davis, J.J., Bueno, P.R., 2013. Biosens. Bioelectron. 50, 437-440.

Fuggle, J. C., Källne, E., Watson, L. M., Fabian, D. J., 1977. Phys. Rev. B 16, 750-761.

Gao, Q., Han, J.M., Ma, Z.F., 2013. Biosens. Bioelectron. 49, 323-328.

Gao, Y.S., Zhu, X.F., Xu, J.K., Lu, L.M., Wang, W.M, Yang, T.T., Xing, H.K., Yu, Y.F., 2016. Anal. Biochem. 500, 80-87.

Gao, Z., Xu, M., Hou, L., Chen, G., Tang, D., 2013. Anal. Chem. 85, 6945-6952.

He, Y., Xie, S.B., Yang, X., Yuan, R., Chai, Y.Q., 2015. ACS Appl. Mater. Interfaces 7, 13360-13366.

Jemal, A., Bray, F., Center, M.M., Ferlay, J., Ward, E., Forman, D., 2011. Ca Cancer J. Clin. 61, 69-90.

Ju, K.Y., Lee, Y., Lee, S., Park, S.B., Lee, J.K., 2011. Biomacromolecules 12, 625-632.

Jung, G., Beck-Sickinger, A.G., 1992. Angew. Chem. Int. Ed. 31, 367-383.

Kaushik, A., Vasudev, A., Ary, S.K., Bhansali, S., 2013. Biosens. Bioelectron. 50, 35-41.

Liu, N., Chen, X., Ma, Z.F., 2013. Biosens. Bioelectron. 48, 33-38.

Liu, Y.L., Ai, K.L., Lu, L.H., 2014. Chem. Rev. 114, 5057-5115.

Liu, Y.Y., Ma, H.M., Gao, J., Wu, D., Ren, X., Yan, T., Pang, X., Wei, Q., 2016. Biosens. Bioelectron. 79, 71-78.

Liu, Z.M., Ma, Z.F., 2013. Biosens. Bioelectron. 46, 1-7.

Mahshid, S. S., Camiré, S., Ricci, F., Vallée-Bélisle, A., 2015. J. Am. Chem. Soc. 137, 15596-15599.

Mellish, K.J., Cox, R.D., Vernon, D.I., Griffiths, J., Brown, S.B., 2002. Photochem. Photobiol. 75, 392-397.

Mohan, K; Donavan, K.C., Arter, J.A., Penner, R.M., Weiss, G.A., 2013. J. Am. Chem. Soc. 135, 7761-7767.

Nam, J. M., Thaxton, C.S., Mirkin, C.A., 2003. Science 301, 1884-1886.

Ou, C.F., Chen, S.H., Yuan, R., Chai, Y.Q., Zhong, X., 2008. J. Electroanal. Chem. 624, 287-292.

Rong, Q.F., Feng, F., Ma, Z.F., 2016. Biosens. Bioelectron. 75, 148-154.

Rong, Q.F., Han, H.L., Feng, F., Ma, Z.F., 2015. Sci. Rep., 5, 11440.

Santos, A., Piccoli, J.P., Santos-Filho, N.A., Cilli, E.M., Bueno P.R., 2015. Biosens. Bioelectron. 68, 281-287.

Sipos, A.J., Urakawa, H., 2016. Lett. Appl. Microbiol. 62, 199-206.

Tang, D.P., Yuan, R., Chai, Y.Q., 2006. Anal. Chim. Acta 564, 158-165

Turner, N. H., & Single, A. M., 1990. Surf. Interface Anal. 15, 215-222.

Walsh, P.C., 2010. J. Urology 183, 1383-1384.

Wang, H.Z., Wang, YZ, Liu, S., Yu, J.H., Guo, Y.N., Xu, Y., Huang, J.D., 2016. Biosens. Bioelectron. 80, 471-476.

Wang, J.L., Munir, A., Li, Z.H, Zhou, H.S., 2010. Talanta 81, 63-67.

Wang, L.Y., Shan, J., Feng, F., Ma, Z.F., 2016. Anal. Chim. Acta 911, 108-113.

Xianyu, Y., Wang, Z., Jiang, X.Y., 2014. Acs Nano 8, 12741-7.

Zhai, D.Y., Liu, B.R., Shi, Y., Pan, L.J., Wang, Y.Q., Li, W.B., Zhang, R., Yu, G.H., 2013. ACS Nano 7, 3540-3546.

Zhai, Q.F., Zhang, X.W., Han, Y.C., Zhai, J.F., Li, J., Wang, E., 2016. Anal. Chem. 88, 945-951.

Zhao, N., He, Y.Q., Mao, X., Sun, Y.H., Zhang, X.B., Li, C.Z., Lin, Y.H., Liu, G.D., 2010. Electrochem. Commun. 12, 471-474.

Zhu, C.Z., Yang, G.H., Li, H., Du, D., Lin, Y.H., 2015. Anal. Chem. 87, 230-249.

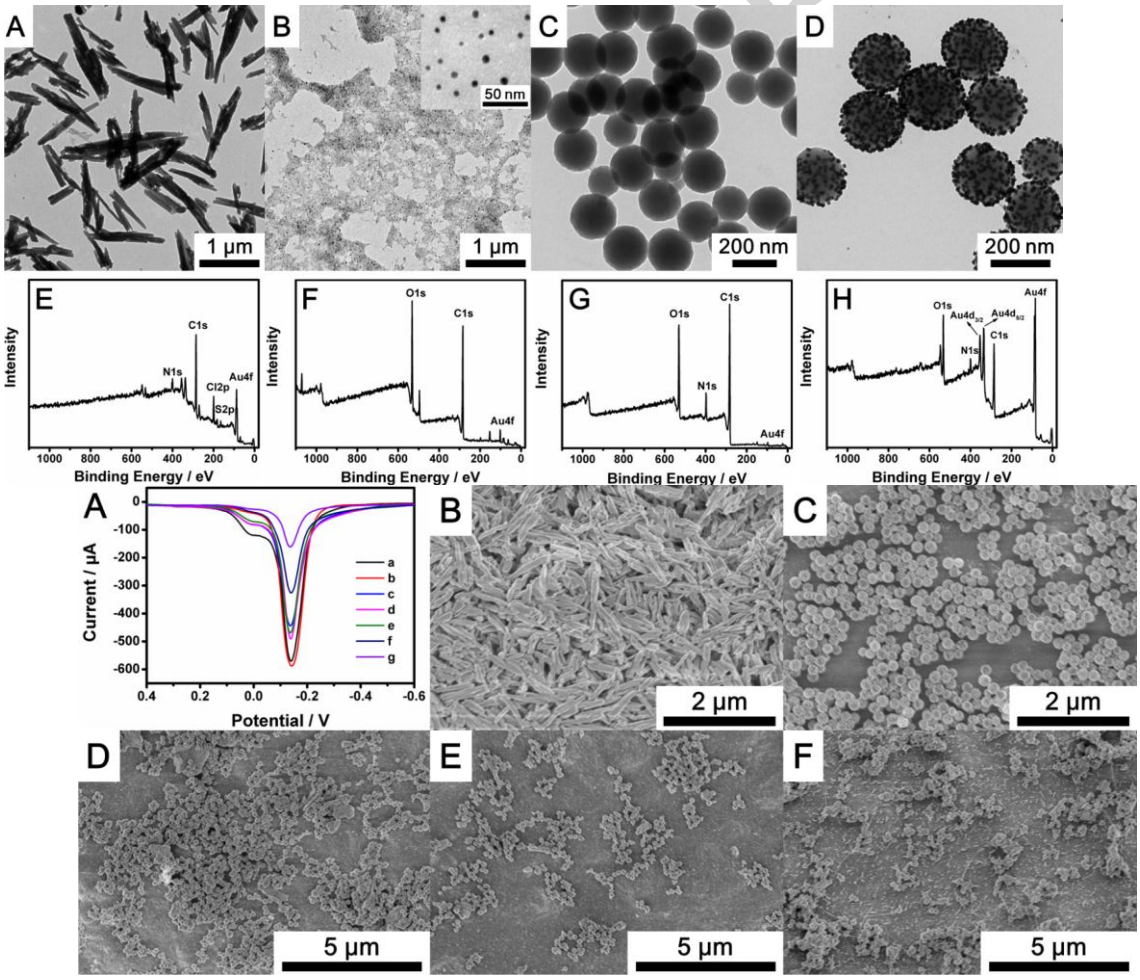

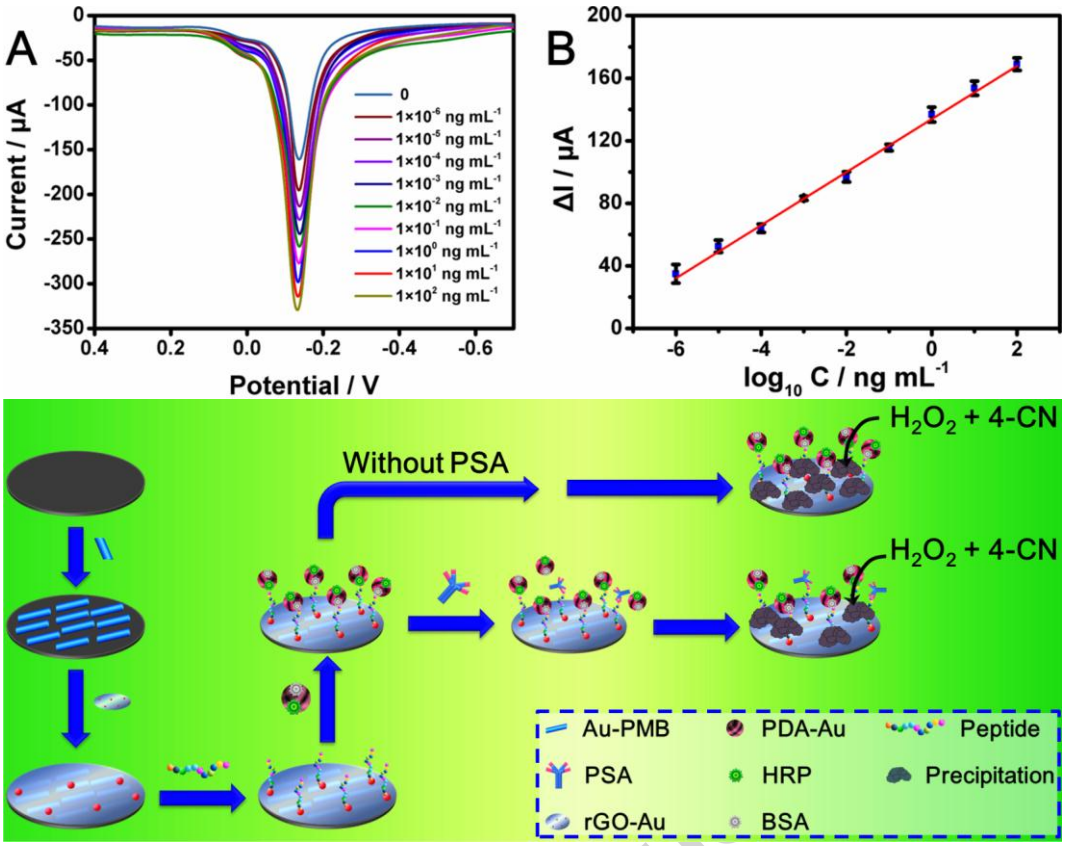

Scheme 1. Schematic illustration of the fabrication procedure and detection principle of the proposed biosensor.

Fig. 1. TEM micrographs of Au-PMB (A), Au-rGO (B), PDA (C) and PDA-Au (D). Inset: magnified TEM micrograph of Au-rGO. XPS survey spectra of Au-PMB (E), Au-rGO (F), PDA (G) and PDA-Au (H).

Fig. 2. SWV responses of the modified electrodes (A) in 0.2 M sodium acetate buffer: Au-PMB/GCE (a), Au-rGO/Au-PMB/GCE (b), peptides/Au-rGO/Au-PMB/GCE (c), PDA-Au-HRP-BSA/peptides/Au-rGO/Au-PMB/GCE before (d) and after incubated with PSA (e) and further treated by enzyme-catalyzed precipitation reaction (f), and

PDA-Au-HRP-BSA/peptides/Au-rGO/Au-PMB/GCE treated by enzyme-catalyzed precipitation reaction without incubating with PSA (g). SEM micrographs of Au-PMB (B), PDA (C), and PDA-Au-HRP-BSA/peptides/Au-rGO/Au-PMB/GCE before (D) and after incubated with PSA (E) and further treated by enzyme-catalyzed precipitation reaction (F).

Fig. 3. (A) SWV responses of the proposed biosensors after incubated with different concentrations of PSA and treated by enzyme-catalyzed precipitation reaction. (B) Linear calibration curve of ΔI and the logarithm of the concentration of PSA.

Highlights

- A new peptide-based biosensor was fabricated for the ultrasensitive detection of prostate specific antigen.
- Au-poly(methylene blue) as a novel redox species were synthesized by oxidative polymerization.
- Polydopamine-Au-horse radish peroxidase nanocomposites were used to accelerate an enzyme-catalyzed precipitation reaction to enhance sensitivity.